# Ion trapping by the graphene electrode in a graphene-ITO hybrid liquid crystal cell

Rajratan Basu[a)] and Andrew Lee
*Department of Physics, Soft Matter and Nanomaterials Laboratory, The United States Naval Academy, Annapolis, Maryland 21402, USA*

(Received 31 July 2017; accepted 9 October 2017; published online 20 October 2017)

A monolayer graphene coated glass slide and an indium tin oxide (ITO) coated glass slide with a planar-aligning polyimide layer were placed together to make a planar hybrid liquid crystal (LC) cell. The free-ion concentration in the LC was found to be significantly reduced in the graphene-ITO hybrid cell compared to that in a conventional ITO-ITO cell. The free-ion concentration was suppressed in the hybrid cell due to the graphene-electrode's ion trapping process. The dielectric anisotropy of the LC was found to increase in the hybrid cell, indicating an increase in the nematic order parameter of the LC due to the reduction of ionic impurities.
https://doi.org/10.1063/1.4998423

Liquid crystals (LCs) generally contain free ions,[1,2] which are generated as impurities during the synthesis process of LCs. Other external factors, such as the LC cell's polyimide (PI) alignment layers[3] and electrodes,[4,5] can also inject free-ion impurities into the LC during the filling process. In electro-optical LC displays (LCDs), the presence of excess ionic impurities triggers several problems, such as slow responses[6] and long-term image sticking effects.[7–12] Therefore, there exists an important research direction to understand the ion transport phenomenon in an LC and the principles governing its subsequent impacts on the LC's electrical, mechanical, and electro-optical properties.[13–21]

Graphene (GP)[22] is a two-dimensional crystalline allotrope of carbon, where the carbon atoms are densely packed in a regular $sp^2$-bonded atomic-scale hexagonal pattern.[23] GP shows high optical transmittance[24] and high conductivity due to ballistic electron transport,[25] and therefore, GP can be used as a transparent electrode in various electro-optic devices.[26–31] In conventional LC cells, the two major components are the LC alignment layers and indium tin oxide (ITO) electrodes. The conventional LC alignment layer is a polyimide (PI)-coated surface where a unidirectional rubbing determines the nematic director profile of the LC in the cell. Here, we report the fabrication of a GP-ITO hybrid LC cell without using any additional PI alignment layer on the graphene-electrode side and show that the free-ion concentration in the hybrid cell is ∼70% less than that in the conventional ITO-ITO LC cell.

The conventional ITO-ITO cell (planar empty cell SA100A200uG180 with a pre-tilt angle of 1.5°, an ITO coated area of 1 $cm^2$, and a spacing of $20 \pm 0.5\,\mu$m) was obtained from *Instec, Inc*. To fabricate the GP-ITO cell, a Chemical Vapor Deposition (CVD) grown monolayer GP film on a copper foil was first obtained from Graphene Supermarket, Inc. The monolayer GP from the copper foil was then transferred onto a $2.5 \times 2.5\,cm^2$ glass substrate using the polymethyl-methacrylate (PMMA) assisted transfer method.[32,33] The sheet resistance of the graphene film on the glass was found to be ∼700 Ω/□. An ITO coated glass slide with a planar-aligning PI substrate (from *Instec, Inc.*) and the GP coated glass substrate were placed together (with the GP film and the PI substrate facing each other) to make a cell with an average thickness of 21 $\mu$m. To make a comparative study, both the ITO-ITO and the GP-ITO cells were filled with E7 ($T_{NI} = 60\,°C$) liquid crystals.

The planar alignment of the LC in both cells was studied by rotating the cells under a crossed polarized microscope. Figure 1(a) schematically shows the ITO layers, PI alignment layers with rubbing, and the nematic LC director ($\hat{n}$) orientation inside the conventional ITO-ITO cell. Figures 1(b) and 1(c) present the micrographs of the LC in the ITO-ITO cell, where $\hat{n}$ is at 45° (bright) and 0° (dark), respectively, with respect to the polarizer. Figure 1(d) shows the picture of the ITO-ITO cell.

The LC molecules can anchor to the *honeycomb* pattern of GP[34,35] or carbon nanotubes,[36–43] employing the $\pi$–$\pi$ electron stacking. Density-functional calculations suggest that this anchoring is reinforced with a binding energy of −2.0 eV by electrostatic energy due to a considerable amount of charge transfer from the LC molecule to the honeycomb pattern[37,38] of the carbon atoms. Figure 1(e) illustrates the $\pi$–$\pi$ stacking interaction that arises due to the overlap of the LC's benzene rings on the GP-honeycomb structure. The LC can achieve a uniform planar-aligned state over a large-scale dimension on GP[28,44,45] due to this strong $\pi$–$\pi$ stacking interaction.[46–49] Therefore, the GP-electrode at one side of the GP-ITO cell can function concurrently as the LC alignment layer as well. The GP-ITO LC cell is schematically presented in Fig. 1(f). Similar to the conventional cell, Figs. 1(g) and 1(h) present the micrographs of the LC in the GP-ITO cell, where $\hat{n}$ is at 45° (bright) and 0° (dark), respectively, with respect to the polarizer. These micrographs confirm the planar alignment of the LC in the GP-ITO cell. Figure 1(i) shows the picture of the GP-ITO cell. To achieve a good electrical contact on the GP surface, an electrically conductive silver epoxy was used as a solder replacement to prevent the GP film from breaking away from the glass slide.

On a single graphene crystalline domain, the LC molecules can assume three different orientations separated by 60° disclination lines due to the hexagonal symmetry of the

a)Electronic mail: basu@usna.edu

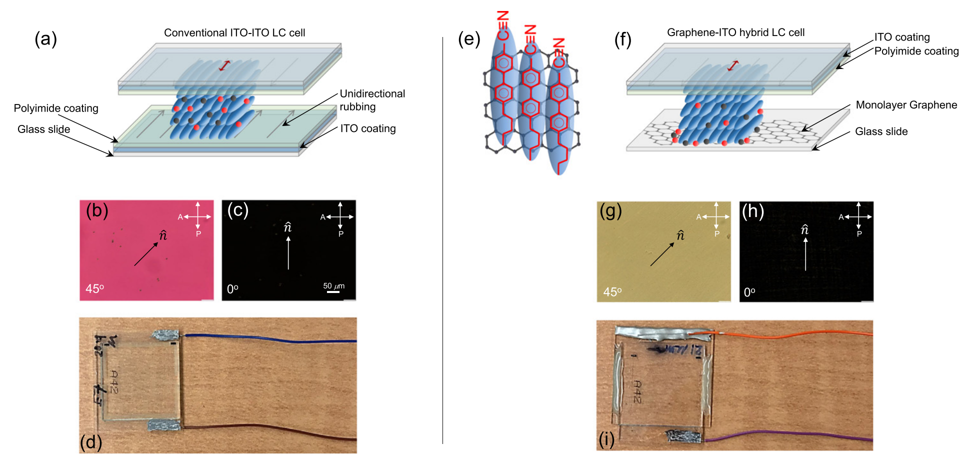


FIG. 1. (a) A schematic representation of a conventional ITO-ITO LC cell containing a layer of ITO and a layer of polyimide with unidirectional rubbing on each glass slide. The *small spheres* represent the ions in the LC. Micrographs of E7 LC in the ITO-ITO cell under the crossed-polarized microscope with the director $\hat{n}$ at (b) 45° (bright) and (c) 0° (dark) with respect to the polarizer. The black dots in micrograph-(b) are 20 μm spacer particles. (d) The picture of a conventional ITO-ITO LC cell. (e) A schematic representation of the alignment of nematic LC molecules on graphene due to $\pi$–$\pi$ electron stacking. The ellipsoids are LCs, and the black honeycomb structure is the graphene surface. The LC molecular structure is shown in the ellipsoid on the graphene surface. The $\pi$–$\pi$ electron stacking is illustrated by matching the LC's benzene rings on the graphene-honeycomb structure. (f) A schematic representation of a graphene-ITO hybrid cell, which contains a monolayer graphene-electrode on one side and a regular ITO-polyimide combination on the other side. It also shows some trapped ions on the GP-electrode, and therefore, fewer ions are present in the LC media. Micrographs of E7 LC in the graphene-ITO cell under the crossed-polarized microscope with $\hat{n}$ at (g) 45° (bright) and (h) 0° (dark) with respect to the polarizer. (i) The picture of a graphene-ITO LC cell. The white bar in micrograph-(c) presents 50 μm.

graphene crystal.[46] The presence of a PI alignment layer at one side of the cell reduces this three-fold degeneracy of the planar orientation of the LC on graphene, and consequently, the LC gains a uniform homogeneous alignment over a large-scale dimension. Using the graphene-electrode (without PI layers) at both sides generates defect-like texture, which results from this alignment degeneracy of LC on graphene.[28] Therefore, we have used the hybrid cell instead of the graphene-electrode at both sides.

The presence of free ions in E7 in the conventional ITO-ITO cell and the hybrid GP-ITO cell was measured by detecting the ion-bump[13,50] in a transient current generated by inverting the voltage across the cell. The nematic phase of an LC shows dielectric anisotropy, $\Delta\varepsilon$, and experiences a torque proportional to $\Delta\varepsilon\, E^2$ (Ref. 51) in an external electric field $E$. Thus, $\hat{n}$ can rotate from the planar to homeotropic configuration above some critical $E$. This reorientation process depends on the *magnitude* of $E$ and not on its *sign*. Therefore, when a constant square wave is applied across a nematic LC cell (i.e., the voltage is inverted at opposite electrodes), the LC molecules do not rotate. However, positive and negative ions in the LC cell are initially separated at opposite electrodes. After the voltage is inverted, the ions start to move towards the opposite electrodes in response to $E$, causing an ion current, $I_{\mathrm{ion}}$, in the cell. When the positive and negative ions meet approximately at the middle of the cell, $I_{\mathrm{ion}}$ reaches its peak value at peak time, $t_{ion-peak} = \frac{d^2}{2\mu E}$, where $\mu$ is the mobility.[13,50] Finally, $I_{\mathrm{ion}}$ drops to zero when the positive ions reach the negative electrode and the negative ions reach the positive electrode of the cell. The total ion transport in the cell can then be calculated by taking the area under the $I_{\mathrm{ion}}$ vs. time curve. A square wave of 30 V at 1 Hz was applied using an Automatic Liquid Crystal Tester (*Instec*, *Inc.*) to detect $I_{\mathrm{ion}}$ for the two cells. The ion concentration, $n_{\mathrm{i}}$ (C m$^{-3}$), was obtained using the cell's known dimensions.

Figures 2(a) and 2(b) show $I_{\mathrm{ion}}$ as a function of time for the conventional ITO-ITO cell and the hybrid GP-ITO cell at $T = 35\,^{\circ}$C and $T = 55\,^{\circ}$C, respectively. Figure 2(c) shows $n_{\mathrm{i}}$ for the two cells as a function of temperature. Figure 2 depicts that $n_{\mathrm{i}}$ is greatly reduced in the GP-ITO hybrid cell.

Several reports in the literature show that the presence of carbon nanomaterials, such as carbon nanotubes,[52–54] graphene,[49,55–59] and fullerenes,[52,60,61] in the LC can significantly reduce the free-ion concentration by the ion-trapping process. In our experiment, the GP-electrode is directly exposed to the LC, as there is no polyimide alignment substrate on GP. Therefore, the GP-electrode traps a significant amount of free ions and reduces the free-ion concentration in the GP-ITO hybrid cell. The ion-trapping process is schematically presented in Fig. 1. The ITO-ITO cell in Fig. 1(a) shows the presence of free ions (both positive and negative) in the LC media. The GP-ITO cell in Fig. 1(f) shows the trapped ions on the GP-electrode, and therefore, fewer ions are present in the LC media.

In another direction, the presence of guest/foreign particles generally introduces disorder in the nematic matrix, decreasing the scalar order parameter, $S(T)$.[62] Free ions also act as foreign charged particles, which are present as impurities in the LC. Therefore, the diminished presence of free ions is expected to increase $S(T)$ in the nematic phase. The nematic phase shows dielectric anisotropy, $\Delta\varepsilon = \varepsilon_{||} - \varepsilon_{\perp}$, where $\varepsilon_{||}$ and $\varepsilon_{\perp}$ are the dielectric components parallel and perpendicular to $\hat{n}$, respectively. An LC's $\Delta\varepsilon \propto S(T)$,[51] and therefore, an enhancement in $\Delta\varepsilon$ indicates an improvement in the orientational order parameter.

We have determined the dielectric behavior of E7 as a function of $E$, at 1000 Hz, in both the cells by the capacitance measurement technique[63] using an Automatic Liquid Crystal Tester (*Instec*, *Inc.*). Figure 3(a) shows the dielectric constant, $\varepsilon$, as a function of $E$ at $T = 30\,^{\circ}$C for both the cells. This shows a typical Fréedericksz transition. Clearly, the LC

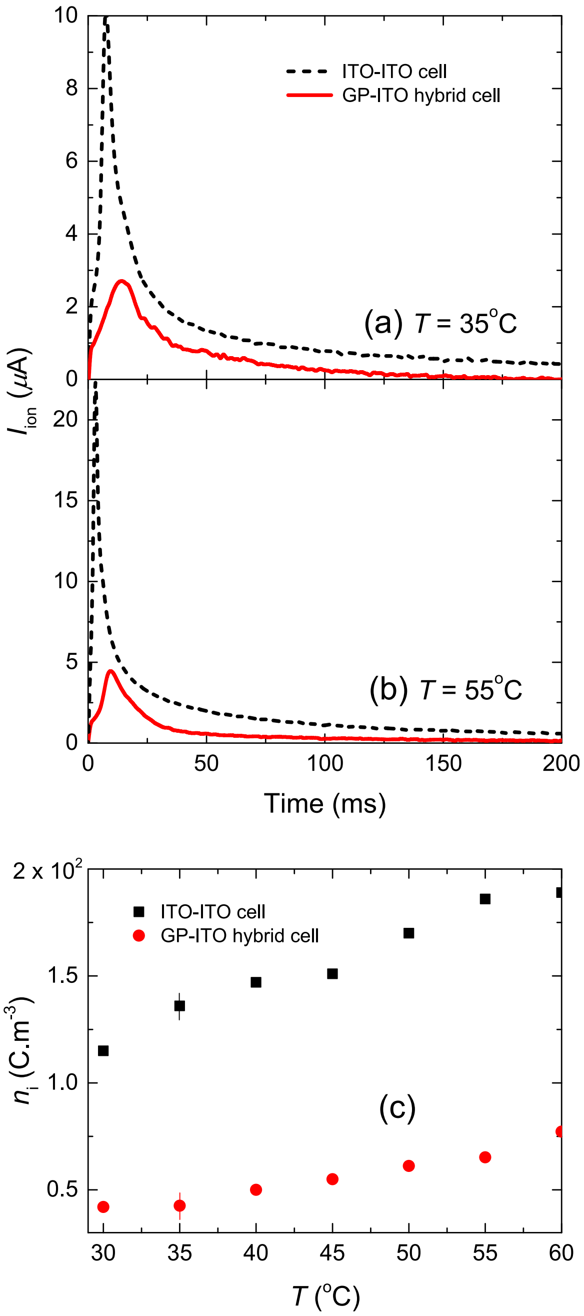


FIG. 2. Ion current, $I_{ion}$, as a function of time for E7 in the two cells at (a) 35 °C and (b) 55 °C, after the voltage is inverted across the cells. The peak represents the ion-bump when positive and negative ions meet approximately at the middle of the cell. (c) Free-ion concentration, $n_i$, as a function of temperature for E7 in the two cells listed. Typical error bars are shown.

in the GP-ITO hybrid cell exhibits a higher $\Delta\varepsilon$ due to the presence of fewer ionic impurities. Figure 3(b) shows that $\Delta\varepsilon$ for E7 remains higher in the GP-ITO hybrid cell in the entire nematic phase. The results suggest that the free-ion reduction improves the orientational order in the LC.

To summarize, we have experimentally demonstrated that in the GP-ITO hybrid cell, the free-ion concentration in E7 is suppressed significantly due to the ion-trapping process by the GP-electrode. This result is important for purifying LCs from excess ions without additional chemical synthesis. The reduction of ionic impurities also leads to a higher $\Delta\varepsilon$ of E7 in the hybrid cell. It is expected that the birefringence of the hybrid cell will also change due to the improved orientational order in the LC. Therefore, our future work involves a systematic study of the birefringence of the LC in the hybrid cell as a function of electric field and temperature.

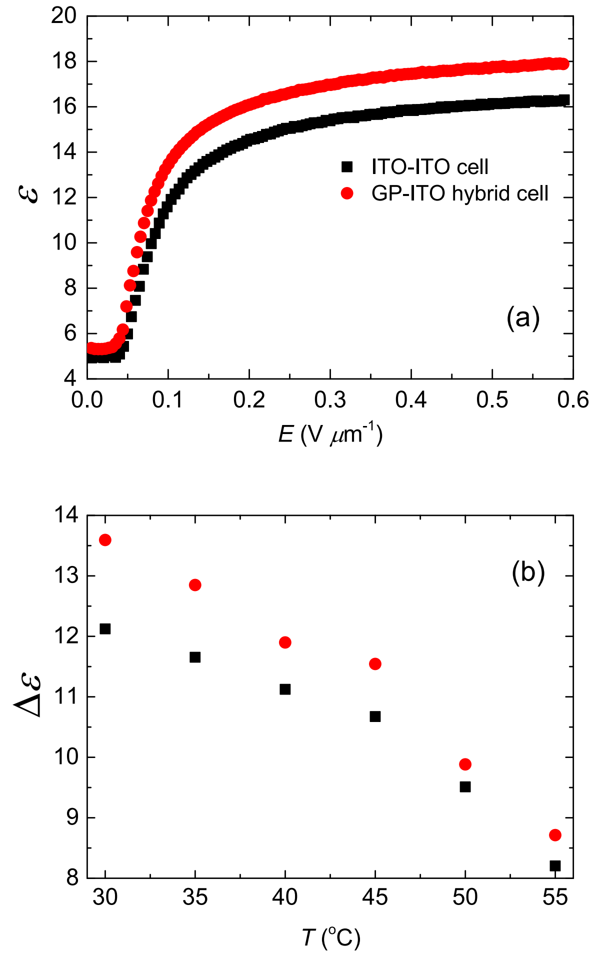


FIG. 3. (a) Dielectric constant, $\varepsilon$, as a function of applied rms field $E$ ($f = 1000$ Hz) in the nematic phase ($T = 30$ °C) of the E7 liquid crystal in two different LC cells listed. This shows that the LC can exhibit a typical Fréedericksz transition in the graphene-ITO hybrid cell. (b) Dielectric anisotropy, $\Delta\varepsilon$, as a function of temperature for E7 in the two cells.

This work was supported by the Office of Naval Research (Award No. N0001417WX01519) and the investment grant at the U.S. Naval Academy.

[1]G. H. Heilmeier and P. M. Heyman, "Note on transient current measurements in liquid crystals and related systems," Phys. Rev. Lett. **18**, 583 (1967).
[2]G. Briere, F. Gaspard, and R. Herino, "Ionic residual conduction in the isotropic phase of a nematic liquid crystal," Chem. Phys. Lett. **9**, 285 (1971).
[3]N. A. J. M. Van Aerle, "Influence of polyimide orientation layer material on the liquid crystal resistivity in LCDs," Mol. Cryst. Liq. Cryst. **257**, 193 (1994).
[4]S. Murakami and H. Naito, "Charge injection and generation in nematic liquid crystal cells," Jpn. J. Appl. Phys., Part 1 **36**, 773 (1997).
[5]S. Naemura and A. Sawada, "Ion generation in liquid crystals under electric field," Mol. Cryst. Liq. Cryst. **346**, 155 (2000).
[6]S. Takahashi, "The investigation of a dc induced transient optical 30-Hz element in twisted nematic liquid-crystal displays," J. Appl. Phys. **70**, 5346 (1991).
[7]H. De Vleeschouwer, B. Verweire, K. D'Have, and H. Zhang, "Electrical and optical measurements of the image sticking effect in nematic LCD'S," Mol. Cryst. Liq. Cryst. **331**, 567 (1999).
[8]H. De Vleeschouwer, F. Bougrioua, and H. Pauwels, "Importance of ion transport in industrial LCD applications," Mol. Cryst. Liq. Cryst. **360**, 29 (2001).

[9]D. Xu, F. Peng, H. Chen, J. Yuan, S.-T. Wu, M.-C. Li, S.-L. Lee, and W.-C. Tsai, "Image sticking in liquid crystal displays with lateral electric fields," J. Appl. Phys. **116**, 193102 (2014).
[10]H. De Vleeschouwer, A. Verschueren, F. Bougrioua, R. van Asselt, E. Alexander, S. Vermael, K. Neyts, and H. Pauwels, "Long-term ion transport in nematic liquid crystal displays," Jpn. J. Appl. Phys., Part 1 **40**, 3272 (2001).
[11]K. H. Yang, "Charge retention of twisted nematic liquid-crystal displays," J. Appl. Phys. **67**, 36 (1990).
[12]N. Sasaki, "A new measurement method for ion density in TFT-LCD panels," Mol. Cryst. Liq. Cryst. **367**, 671 (2001).
[13]R. Basu and A. Garvey, "Effects of ferroelectric nanoparticles on ion transport in a liquid crystal," Appl. Phys. Lett. **105**, 151905 (2014).
[14]K. Neyts, S. Vermael, C. Desimpel, G. Stojmenovik, R. van Asselt, A. R. M. Verschueren, D. K. G. de Boer, R. Snijkers, P. Machiels, and A. van Brandenburg, "Lateral ion transport in nematic liquid-crystal devices," J. Appl. Phys. **94**, 3891 (2003).
[15]M. Yamashita and Y. Amemiya, "Drift mobility of positive ions in nematic MBBA at low electric field," Jpn. J. Appl. Phys., Part 1 **17**, 1513 (1978).
[16]V. Novotny, "Measurement of mobilities of particles in liquids by optical and electrical transients," J. Appl. Phys. **50**, 2787 (1979).
[17]A. Sugimura, N. Matsui, Y. Takahashi, H. Sonomura, H. Naito, and M. Okuda, "Transient currents in nematic liquid crystals," Phys. Rev. B **43**, 8272 (1991).
[18]H. Naito, M. Okuda, and A. Sugimura, "Transient discharging processes in nematic liquid crystals," Phys. Rev. A **44**, R3434 (1991).
[19]H. Naito, K. Yoshida, and M. Okuda, "Transient charging current in nematic liquid crystals," J. Appl. Phys. **73**, 1119 (1993).
[20]C. Colpaert, B. Maximus, and A. De Meyere, "Adequate measuring techniques for ions in liquid crystal layers," Liq. Cryst. **21**, 133 (1996).
[21]A. Sawada, A. Manabe, and S. Nameura, "A comparative study on the attributes of ions in nematic and isotropic phases," Jpn. J. Appl. Phys., Part 1 **40**, 220 (2001).
[22]K. S. Novoselov, A. K. Geim, S. V. Morozov, D. Jiang, Y. Zhang, S. V. Dubonos, I. V. Grigorieva, and A. A. Firsov, "Electric field effect in atomically thin carbon films," Science **306**, 666 (2004).
[23]J. C. Meyer, A. K. Geim, M. I. Katsnelson, K. S. Novoselov, T. J. Booth, and S. Roth, "The structure of suspended graphene sheets," Nature **446**, 60 (2007).
[24]R. R. Nair, P. Blake, A. N. Grigorenko, K. S. Novoselov, T. J. Booth, T. Stauber, N. M. R. Peres, and A. K. Geim, "Fine structure constant defines visual transparency of graphene," Science **320**, 1308 (2008).
[25]A. K. Geim and K. S. Novoselov, "The rise of graphene," Nat. Mater. **6**, 183 (2007).
[26]P. Blake, P. D. Brimicombe, R. R. Nair, T. J. Booth, D. Jiang, F. Schedin, L. A. Ponomarenko, S. V. Morozov, H. F. Gleeson, E. W. Hill, A. K. Geim, and K. S. Novoselov, "Graphene-based liquid crystal device," Nano Lett. **8**, 1704 (2008).
[27]X. Wang, L. Zhi, and K. Mullen, "Transparent, conductive graphene electrodes for dye-sensitized solar cells," Nano Lett. **8**, 323 (2008).
[28]R. Basu and S. Shalov, "Graphene as transmissive electrodes and aligning layers for liquid-crystal-based electro-optic devices," Phys. Rev. E **96**, 012702 (2017).
[29]Y. U. Junga, K. W. Parka, S. T. Hura, S. W. Choia, and S. J. Kanga, "High-transmittance liquid-crystal displays using graphene conducting layers," Liq. Cryst. **41**, 101 (2014).
[30]V. Marinova, Z. F. Tong, S. Petrov, S. H. Lin, M. S. Chen, Y. H. Lin, Y. C. Lai, P. Yu, and K. Y. Hsu, "Liquid crystal cell with graphene electrodes," J. Phys.: Conf. Ser. **794**, 012009 (2017).
[31]J. Guo, C. M. Huard, Y. Yang, Y. Jae Shin, K.-T. Lee, and L. J. Guo, "ITO-free, compact, color liquid crystal devices using integrated structural color filters and graphene electrodes," Adv. Opt. Mater. **2**, 435 (2014).
[32]X. Li, Y. Zhu, W. Cai, M. Borysiak, B. Han, D. Chen, R. D. Piner, L. Colombo, and R. S. Ruoff, "Transfer of large-area graphene films for high-performance transparent conductive electrodes," Nano Lett. **9**, 4359 (2009).
[33]X. Liang, B. A. Sperling, I. Calizo, G. Cheng, C. A. Hacker, Q. Zhang, Y. Obeng, K. Yan, H. Peng, Q. Li, X. Zhu, H. Yuan, A. R. H. Walker, Z. Liu, L.-M. Peng, and C. A. Richter, "Toward clean and crackless transfer of graphene," ACS Nano **5**, 9144 (2011).
[34]D. W. Kim, Y. H. Kim, H. S. Jeong, and H.-T. Jung, "Direct visualization of large-area graphene domains and boundaries by optical birefringency," Nat. Nanotechnol. **7**, 29 (2012).
[35]M. A. Shehzad, D. H. Tien, M. W. Iqbal, J. Eom, J. H. Park, C. Hwang, and Y. Seo, "Nematic liquid crystal on a two dimensional hexagonal lattice and its application," Sci. Rep. **5**, 13331 (2015).
[36]I.-S. Baik, S. Y. Jeon, S. H. Lee, K. A. Park, S. H. Jeong, K. H. An, and Y. H. Lee, Appl. Phys. Lett. **87**, 263110 (2005).
[37]K. A. Park, S. M. Lee, S. H. Lee, and Y. H. Lee, "Anchoring a liquid crystal molecule on a single-walled carbon nanotube," J. Phys. Chem. C **111**, 1620 (2007).
[38]S. Y. Jeon, K. A. Park, I. S. Baik, S. J. Jeong, S. H. Jeong, K. H. An, S. H. Lee, and Y. H. Lee, "Dynamic response of carbon nanotubes dispersed in nematic liquid crystal," Nano **2**, 41 (2007).
[39]R. Basu and A. Garvey, "Insulator-to-conductor transition in liquid crystal-carbon nanotube nanocomposites," J. Appl. Phys. **120**, 164309 (2016).
[40]R. Basu and G. S. Iannacchione, "Nematic anchoring on carbon nanotubes," Appl. Phys. Lett. **95**, 173113 (2009).
[41]R. Basu and G. S. Iannacchione, "Orientational coupling enhancement in a carbon nanotube dispersed liquid crystal," Phys. Rev. E **81**, 051705 (2010).
[42]R. Basu, C.-L. Chen, and C. Rosenblatt, "Carbon nanotube-induced macroscopic helical twist in an achiral nematic liquid crystal," J. Appl. Phys. **109**, 083518 (2011).
[43]R. Basu, C. Rosenblatt, and R. Lemieux, "Chiral induction in thioester and oxoester liquid crystals by dispersed carbon nanotubes," Liq. Cryst. **39**, 199 (2012).
[44]R. Basu, D. Kinnamon, and A. Garvey, "Graphene and liquid crystal mediated interactions," Liquid Crystals **43**, 2375 (2016).
[45]R. Basu, "Enhancement of polar anchoring strength in a graphene-nematic suspension and its effect on nematic electro-optic switching," Phys. Rev. E **96**, 012707 (2017).
[46]R. Basu, D. Kinnamon, N. Skaggs, and J. Womack, "Faster in-plane switching and reduced rotational viscosity characteristics in a graphene-nematic suspension," J. Appl. Phys. **119**, 185107 (2016).
[47]R. Basu, D. Kinnamon, and A. Garvey, "Detection of graphene chirality using achiral liquid crystals," J. Appl. Phys. **118**, 114302 (2015).
[48]R. Basu, D. Kinnamon, and A. Garvey, "Nano-electromechanical rotation of graphene and giant enhancement in dielectric anisotropy in a liquid crystal," Appl. Phys. Lett. **106**, 201909 (2015).
[49]R. Basu, "Effects of graphene on electro-optic switching and spontaneous polarization of a ferroelectric liquid crystal," Appl. Phys. Lett. **105**, 112905 (2014).
[50]Z. Zou, N. A. Clark, and M. A. Handschy, "Ionic transport effects in SSFLC cells," Ferroelectrics **121**, 147 (1991).
[51]P. G. De Gennes and J. Prost, *The Physics of Liquid Crystals* (Oxford University Press, New York, 1994).
[52]C.-W. Lee and W.-P. Shih, "Quantification of ion trapping effect of carbon nanomaterials in liquid crystals," Mater. Lett. **64**, 466 (2010).
[53]H. Y. Chen, W. Lee, and N. A. Clark, "Faster electro-optical response characteristics of a carbon-nanotube-nematic suspension," Appl. Phys. Lett. **90**, 033510 (2007).
[54]R. Basu, "Effect of carbon nanotubes on the field-induced nematic switching," Appl. Phys. Lett. **103**, 241906 (2013).
[55]R. Basu, A. Garvey, and D. Kinnamon, "Effects of graphene on electro-optic response and ion-transport in a nematic liquid crystal," J. Appl. Phys. **117**, 074301 (2015).
[56]P.-W. Wu and W. Lee, "Phase and dielectric behaviors of a polymorphic liquid crystal doped with graphene nanoplatelets," Appl. Phys. Lett. **102**, 162904 (2013).
[57]P.-C. Wu, L. N. Lisetski, and W. Lee, "Suppressed ionic effect and low-frequency texture transitions in a cholesteric liquid crystal doped with graphene nanoplatelets," Opt. Express **23**, 11195 (2015).
[58]Y. Garbovskiy and I. Glushchenko, "Nano-objects and ions in liquid crystals: Ion trapping effect and related phenomena," Crystals **5**, 501 (2015).
[59]D. P. Singh, S. K. Gupta, T. Vimal, and R. Manohar, "Dielectric, electro-optical, and photoluminescence characteristics of ferroelectric liquid crystals on a graphene-coated indium tin oxide substrate," Phys. Rev. E **90**, 022501 (2014).
[60]W. Lee, C.-Y. Wang, and Y.-C. Shih, "Effects of carbon nanosolids on the electro-optical properties of a twisted nematic liquid-crystal host," Appl. Phys. Lett. **85**, 513 (2004).
[61]R. K. Shukla, K. K. Raina, and W. Haase, "Fast switching response and dielectric behavior of fullerene/ferroelectric liquid crystal nanocolloids," Liq. Cryst. **41**, 1726 (2014).
[62]M. Caggioni, A. Roshi, S. Barjami, F. Mantegazza, G. S. Iannacchione, and T. Bellini, "Isotropic to nematic transition of aerosil-disordered liquid crystals," Phys. Rev. Lett. **93**, 127801 (2004).
[63]R. Basu and G. Iannacchione, "High-resolution dielectric spectroscopy and electric-field dependence of carbon allotropes including multiwall and single-wall nanotubes," Appl. Phys. Lett. **92**, 052906 (2008).